

Final Draft
of the original manuscript:

Boecking, A.; Koleva, V.; Wind, J.; Thiermeyer, Y.; Blumenstein, S.; Goebel, R.; Skiborowski, M.; Wessling, M.:

Can the variance in membrane performance influence the design of organic solvent nanofiltration processes?

In: Journal of Membrane Science. Vol. 575 (2019) 217 - 228.

First published online by Elsevier: 31.12.2018

<https://dx.doi.org/10.1016/j.memsci.2018.12.077>

Can the variance in membrane performance influence the design of organic solvent nanofiltration processes?

Axel Böcking^a, Velichka Koleva^b, Jan Wind^c, Yvonne Thiermeyer^{d,e},
Stefanie Blumenschein^e, Rebecca Goebel^d, Mirko Skiborowski^d, Matthias
Wessling^{a,f}

^a*Chemical Process Engineering - AVT.CVT, RWTH Aachen University, Forckenbeckstr.
51, 52074 Aachen, Germany*

^b*Evonik Resource Efficiency GmbH, Paul-Baumann-Str. 1, 45772 Marl, Germany*

^c*Helmholtz-Zentrum Geesthacht, Institute for Polymer Research, Max-Planck-Str. 1,
21502 Geesthacht, Germany*

^d*TU Dortmund University, Department of Biochemical and Chemical Engineering,
Laboratory of Fluid Separation, Emil-Figge-Str. 70, 44227 Dortmund, Germany*

^e*Merck KGaA, Frankfurter Str. 250, 64293 Darmstadt, Germany*

^f*DWI-Leibniz Institute for Interactive Materials, Forckenbeckstr. 50, 52074
Aachen, Germany*

Abstract

The development of organic solvent nanofiltration (OSN) membranes has been a continuous effort during the past decade. Several groups generated and published experimental results and simulations with either tailor-made membranes or industrial products. The published data space is diverse, with a single publication often focusing on a certain membrane only, a group of specific solutes only, on the effect of solvent only. A comprehensive comparison of all of these is still lacking. An analysis on the reliability of quantified transport parameters is missing, in particular when different analysis methods and different membrane systems are used. The technology is in its incubation phase with a need for reliable data and measurement standards to ground the process design on reliable membrane transport properties. This

study uses an unprecedented extensive standard experimental procedure to measure separation characteristics of polymer membranes for the separation of organic solutes from organic solvents.

For a variety of different solvents, solutes and membranes, flux and retention measurements are rigorously characterized by round robin tests at different labs using different analytical systems. This extensive collaborative study evaluates for the first time which fluctuations in results occur under comparable conditions of lab-scale experiments at different locations and which influence these have on the design of OSN processes.

Utilizing the variance in the membrane transport data, a process design study and optimization is presented. For the first time ever, we report how variance in membrane transport properties can influence the process design ranging from a simple single stage system for values for the upper transport limits, to a two stage system with a permeate recirculation for mean values, to a complex three stage system for the lower limits.

Keywords: Organic solvent nanofiltration, Solvent resistant nanofiltration, Experimental standardized procedure, Statistical comparison, Functional membrane characterization

1. Introduction

2 Taking membrane research from its initial phase of concept development,
3 material and membrane design into process development requires substantial
4 resources and time. This is not special but true for many innovations starting
5 with an innovation trigger. This is also known as the Gartner Hype Cycle
6 [1]. Judgment of the quality of the innovation trigger occurs often through

7 reproducibility and applications studies and generally also creates - after a
8 peak of inflated expectations - a trough of disillusion.

9 In membrane research, the innovation trigger is assumed to occur through
10 the availability of new materials and membranes made thereof. Yet, it is of-
11 ten not well known how statistically significant the mass transport properties
12 of new membrane materials and new membrane products are. In a recent
13 meta-study for example [2], published in this journal with more than 3000 ref-
14 erences, the authors pose the fundamental questions (a) whether there is an
15 average proton conductivity for Nafion membranes, (b) how the proton con-
16 ductivity due to Nafion modification has evolved over past 10 years, (c) which
17 additives really contribute to a conductivity increase, (d) how temperature
18 or humidity affect conductivity. While such questions are not scientifically
19 inspiring and do not initiate a new hype cycle, such questions are important
20 in order to understand and judge the significance of a new material or mem-
21 brane type. Here we pose similar questions with respect to the statistical
22 significance and comparability of characterization methods to quantify mass
23 transport properties for membranes used in organic solvent nanofiltration.
24 As opposed to the meta-study, we have chosen to engage different labs and
25 research groups with comparable analytical infrastructure, to use a round-
26 robin test evaluating the results of a developed standard experimental proce-
27 dure. This leads to conclusions on standard deviations in flux and retention
28 values in a complex parameter space for different membrane materials in
29 various solvent/solute systems.

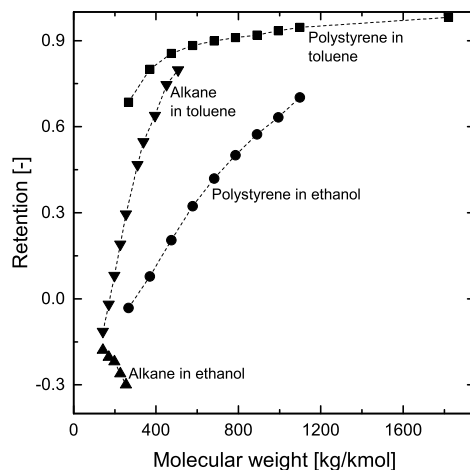


Figure 1: Retention measurements using different solvents and solutes for PuraMem[®] S600 at 30 bar and 25 °C show different behaviour of the membrane.

30 2. Background

31 Organic solvent nanofiltration (OSN) became a new member of the family
 32 of pressure-driven membrane processes by the discovery of solvent resistant
 33 membranes. Up to now, a great number of various applications were devel-
 34 oped since the production and reactions in organic solvents comprises a wide
 35 range [3, 4]. Although OSN is still in the focus of industry as an energy-
 36 efficient separation process, there are only a few established plants [5–7].
 37 However, the progress in the investigation of this field is still growing, and
 38 the challenges include a wide spectrum of different issues. For instance, the
 39 community knows that flux and retention depends on the interaction of so-
 40 lutes, solvents, and membranes [8–14]. Stamatialis et al. [15] suggested a
 41 three-dimensional space of properties determining the mass transport prop-
 42 erties of solvent and solute transport.

43 Due to this complex interplay, the molecular weight cut off (MWCO),

44 defined as the molecular weight that is rejected by 90 %, also depends on the
45 system of compounds. Figure 1 shows retention curves for PuraMem[®] S600
46 at 30 bar in two different solvents using two different solutes. It demonstrates
47 the strong dependence of the functional membrane characteristic on the used
48 compounds.

49 Nevertheless, the MWCO is measured and determined for OSN mem-
50 branes in many different ways, and no standard test system is established
51 [16–19]. See Toh et al. [20] proposed first to standardize the method for a
52 membrane characterization measurement of the MWCO in OSN. The idea
53 was to use a homologous series of polystyrene oligomers which are soluble in
54 many organic solvents to find the MWCO and possibly recognize leak flux.
55 In fact, lot of data can be found in the literature for commercially available
56 and new developed membranes [21]. These data are commonly presented as
57 individual or a few measurements, and often it is not stated if the data are
58 reproducible.

59 This diversity of methods and lack of information about comparability
60 and reproducibility is delicate for research as well as an industrial applica-
61 tion of the technology, since it complicates and delays a possible commer-
62 cialization of new membranes. In addition, it poses a risk to process design
63 since data for specific products have to be retested and evaluated. Thus, the
64 expansion of OSN plants in real processes slows down and turns out of focus
65 of the process designer. However, Schmidt et al. [22] have offered a process
66 design workflow for general new OSN processes, and there exist manuals to
67 support membrane experiments for process design [23]. These approaches
68 are indeed steps towards a higher acceptance of OSN in industry, though

69 we still owe a proof of accuracy for results from membrane characterization
70 experiments. Also, Shi et al. [24] conclude that new research in module and
71 process design is necessary besides new membrane materials to achieve for
72 example ultra-high permeance. Marchetti et al. [25] point out the selectiv-
73 ity challenge in OSN and suggest that process engineering solutions lead to
74 a need of standardized procedures for membrane characterization. In their
75 general review of data quality, Keller et al. [26] highlight the importance of
76 data quality and especially accuracy and precision as important elements for
77 a correct interpretation and evaluation of experimental results.

78 In order to achieve this aim and to follow the recommendations of [24] and
79 [25], a consortium of research groups and industrial partners has been formed,
80 working on a comparison and validation of experimental results. The main
81 objective of this consortium is to define and assess a standard experimental
82 procedure for several chemical systems. The standardized procedure should
83 enable an estimation to determine whether (new) membranes/materials are
84 suitable for process design. For this purpose, results for a membrane must
85 ideally exist for a similar chemical model system. We categorized the sol-
86 vents and solutes to combine ideal model systems. The results from the
87 experimental plan ought to be comparable and reliable between different in-
88 stitutions. Therefore, we performed extensive round robin testing to show
89 for the first time the comparability and reliability of such measurements
90 by cooperative experiments. Subsequently, we evaluated the results of the
91 standardized procedure with statistical methods. Furthermore, additional
92 bilateral cooperative tests were performed for other chemical systems and
93 evaluated accordingly as well. During the development of the standardized

94 procedure different sources for occurring errors, caused e.g. by the different
95 analytic methods, were identified and ruled out. For an evaluation of the
96 comparability of the measurements at the different locations, a statistical
97 analysis is indispensable to avoid arbitrary criteria. The error estimation en-
98 ables end-users to select suitable membranes more quickly. Besides, it allows
99 membrane manufacturers to judge faster whether it is economically viable to
100 bring newly developed membranes to production. The present work is con-
101 sequently of major importance for the transfer of research results in the field
102 of membrane development to later processes and the evaluation in industry.
103

104 **3. Experimental standard measurement procedure**

105 *3.1. Materials and categorization*

106 An appropriate categorization usable for test systems has to be as simple
107 as possible and as accurate as necessary. Following this maxim, we decided to
108 categorize the solvents in protic and non-protic solvents. In protic solvents,
109 we extended the category with two degrees of polarity and for non-protic
110 solvents with three degrees of polarity. Therefore, the normalized polarity
111 index of Reichardt [32] supplies the values. The same as the polarity, in this
112 way a wide range of the Hansen-Solubility parameter [28] and the relative
113 permittivity [27] is covered. Overall, six solvents were chosen to define the
114 set of ideal test-solvents (Table 1), of which ethanol and toluene were used
115 as solvents in the round robin tests. The purity of all solvents used is ACS
116 grade. The supplier of the solvents could be chosen individually by the con-
117 tributors.

Table 1: Properties of the selected test solvents for the experimental standardized procedure [27, 28].

Solvent	Hansen Solubility Parameter						Polarity	Category
	δ_{tot}	δ_d	δ_p	δ_h	ϵ_r	E_T^N [%]		
Ethanol (EtOH)	26.52	15.8	8.8	19.4	22.4	65.4	protic-polar	
Isopropyl alcohol (IPA)	23.58	15.8	6.1	16.4	18.3	54.6	protic-moderate polar	
Butanone (MEK)	19.05	16.0	9.0	5.1	18.5	32.7	aprotic-polar	
Ethyl acetate (ESTP)	18.15	15.8	5.3	7.2	6.02	23	aprotic-moderate polar	
Toluene	18.16	18.0	1.4	2.0	2.38	9.9	aprotic-nonpolar	
n-Heptane	15.3	15.3	0.0	0.0	1.92	1.2	aprotic-nonpolar	

Table 2: Properties of the selected test solutes for the experimental standardized procedure [16, 29–31].

Solute group (Category)	Selected exam- ples	Mw [kg/kmol]	Structure	Polarity	Branch of indus- try
n-Alkane	Decane - Hexatriacontane	ca. 140 - 500	Linear	Nonpolar	Petrochemistry
Sugar and Derivative sugar	Sucrose octaac- etate (SOA)	677	Branched out widely	Moderate polar	Food- and agricultural chemistry
Polymer	Polystyrene (PS), Poly-(methyl methacrylate) (PMMA)	ca. 200 - 2000	Linear	PS: nonpo- lar PMMA: moderate polar	Commodity chemicals and polymer chem- istry

118 The categorization of solutes is much more complicated than for the sol-
119 vents because of the multitude of possible compounds and functional groups.
120 Additional to a classification of the structure, polarity and molecular weight,
121 it is beneficial to give the branch of industry in which the solutes and related
122 solutes are often used. Supplementary, we take solubility, analyzability, and
123 costs into account. Thereby, the solute groups are chosen in such a way that
124 either MWCO curves or individual retention as indicator for estimations on
125 real substances can be measured.

126 Table 2 shows three solute groups defined with the solute properties for
127 the ideal test systems. All solute substances used are of ACS grade pu-
128 rity. The contributors used as solutes in the round robin tests polystyrene
129 oligomer mixtures containing PSS-ps560 and PSS-ps1.8k (Polymer Standards
130 Service GmbH, Mainz, Germany) with a molar mass distribution from 266
131 to 1800 kg/kmol. The bilateral cooperative test systems consisted of these
132 polystyrene oligomers in the remaining solvents from Table 1 as well as
133 n-alkanes (Thermo Fisher Scientific Inc.) and sucrose octaacetate (SOA)
134 (Merck KGaA) in each solvent and poly-(methyl methacrylate) (Polymer
135 Standards Service GmbH) in each solvent. We selected the solute combina-
136 tions concerning solubility and simple analysis assuming that solute/solute
137 interactions have no significant influence on the measurements [33].

138 The OSN membranes can be distinguished in terms of membrane ma-
139 terial and membrane type [3]. For the standard measurement procedure
140 development, we focused on polymeric membranes and tested several inte-
141 grally skinned asymmetric membranes as well as some thin film composite
142 membranes. Four different membranes were used in the round robin test by

143 each contributor: DuraMem[®] 200 and 300 (polyimide-based membranes),
144 PuraMem[®] S600 and a PDMS membrane (both with silicone-based separa-
145 tion layer). DuraMem[®] and PuraMem[®] membranes are products of Evonik
146 Resource Efficiency GmbH and the Helmholtz-Zentrum Geesthacht provided
147 the PDMS membrane. The membranes with a polyimide-based separation
148 layer are suitable for applications in polar solvents (e.g. ethanol) whereas
149 the silicone-based membranes are more appropriate for nonpolar solvents
150 (e.g. toluene). Therefore, the particular membranes selection covers a broad
151 range of possible membrane uses (e.g. solvents and solutes with different
152 physico-chemical properties).

153 While the different partners were performing the same experiments, there
154 were important differences in the experimental set-ups and the analytical
155 methods. Some set-ups are commercially available (e.g., METcell cross flow
156 set-up from Evonik Resource Efficiency GmbH), some are tailor-made by an
157 equipment manufacturer, and one is self-constructed. Therefore, membrane
158 test cells with different geometry (round cells, rectangle cells) and scale were
159 applied throughout the tests. The active membrane areas used vary between
160 50 and 100 cm² per module. Test system volume, control instruments (pres-
161 sure, temperature, flow) and analytical devices were various too. This is
162 representative for the diversity that is present not only in the scientific com-
163 munity, but also in industrial laboratories. The diversity brings, naturally, a
164 high number of important factors that can potentially contribute to differ-
165 ences in the experimental results. Such results might even lead to different
166 conclusions. Therefore, it is indispensable to implement a standard measure-
167 ment procedure, as well as to evaluate the variance in the obtained results,

168 as has been done in the scope of the current study.

169 *3.2. Experimental standardized procedure*

170 All contributors unified the measurement procedure together. At least
171 two identical membrane coupons were tested at the desired conditions. Us-
172 ally the testing cells were connected in parallel. The DuraMem[®] and PuraMem[®]
173 membranes were pre-washed using the process solvent until 5 ml cm⁻² perme-
174 ate was collected or permeate became colorless. This procedure is necessary
175 to prepare the membrane for its use, by removing the conditioning agent from
176 its surface. Furthermore, the solvent treatments of the membranes have to
177 be equal since they have a major impact on the membrane performance [34].
178 The membrane performance was determined by measuring the pure solvent
179 permeate flux and the retention of different molecules (markers) in different
180 solvents.

181 Figure 2 illustrates the agreed process conditions of the experimental
182 standardized procedure. The pure solvent flux measurements were carried
183 out at a pressure of 20 bar and 30 bar, a temperature of around 25 °C and
184 a cross-flow velocity of 1 m s⁻¹. Flux was measured by collecting 5 ml of
185 permeate sample. The amount of collected permeate was controlled with a
186 mass balance (especially important by low permeate flux and high volatile
187 solvent). Also, measured flux values of electronic flow meters were validated
188 by this method.

189 For the retention measurements, samples were taken at the same process
190 conditions as in the permeation measurements. The process pressure was se-
191 quentially increased (20-30-40 bar) whereby permeate and retentate samples
192 were taken at the end of each pressure step. The solute concentration in the

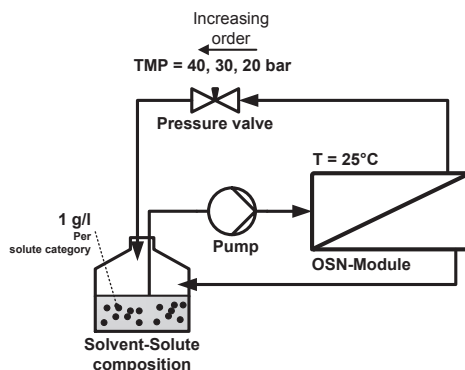


Figure 2: Schematic illustration of the experimental standardized procedure.

193 feed mixtures was kept constant during the experiments (continues permeate
 194 return) at a maximum of 1 g L^{-1} for each used solute group.

195 Following the membrane manufacturer recommendation, polyimide-
 196 based membranes were operated under pressure for 4 h before taking samples
 197 for flux and retention measurements. The time is required for the membrane
 198 to reach the steady state of its performance and abating representative re-
 199 sults accordingly. When silicone-based membranes were applied, the time
 200 for compaction was set to 2 h. Permeate and retentate samples were taken
 201 simultaneously to determine the membrane retention. The retention was
 202 calculated by:

$$R_i = 1 - \frac{c_i (\text{Permeate})}{c_i (\text{Retentate})} \quad (1)$$

203 3.3. Analytic methods

204 Evonik, Merck and TU Dortmund University applied the high-performance
 205 liquid chromatography (HPLC-method) described by See Toh et al. [20] after
 206 all round robin tests and for tests with Poly-(methyl methacrylate) (PMMA).
 207 The existing facilities of the partners were used. The used HPLC device at

208 Merck KGaA, for example, is an HPLC Hitachi LaChrom (Hitachi High Tech-
209 nologies America, Illinois, USA) equipped with an UV-vis detector. RWTH
210 Aachen University and the Helmholtz-Zentrum Geesthacht (HZG) used a
211 gel permeation chromatography (GPC) method to determine the concen-
212 trations of the polystyrene oligomers and PMMA. The GPC were executed
213 with a UV/vis detector and minimum two columns (SDV, 100 Å pore size,
214 3 µm particles, 8.0x300mm (IDxlength), Polymer Standards Service GmbH,
215 Mainz, Germany). Tetrahydrofuran (AnalaR) was used as mobile phase, and
216 the UV detector was set at the same wavelength as in the HPLC-method (264
217 nm). The solvent had to be evaporated from the samples before analysis, and
218 the solutes had to be re-dissolved in the mobile phase. These steps were car-
219 ried out in a very cautious way (evaporating at low temperature, accurate
220 re-dissolving) to minimize loss of solute. Samples from tests with alkanes
221 and sugar were analyzed by gas chromatography as described by Postel et al.
222 [16]. The used GC device is dependent on the contributor. At RWTH, for
223 example, a GC 6890 system (Agilent, CA, USA) with liquid autosampler and
224 flame ionization detector (FID) was used. An Agilent 19091J-413 HP-5 col-
225 umn was used coated with 5 % phenyl methyl siloxane, 30 m length, 0.32 mm
226 inner diameter and 0.25 mm thickness.

227 In order to compare the analytical technique used by the partners, they
228 mutually exchange samples (permeate and retentate) during the experimen-
229 tal phase and re-analyze these in their laboratory. The resulting retention
230 curves were compared and an analytical error was calculated.

231 4. Statistical analysis and evaluation

232 While it is often stated that comparable results have been obtained in dif-
233 ferent studies, these statements are qualitative and therefore subjective. To
234 avoid such subjectivity and allow for a meaningful quantitative reference, we
235 considered a statistical evaluation of the results. Thus, we defined a degree
236 of congruence. The difference between a random sample and a reference or
237 confidence intervals compared to each other are typically used. Confidence
238 intervals should give the precision of an estimated value. However, real val-
239 ues for flux or solute retention cannot be determined because of the limited
240 influenceable structure of membranes.

241 We considered confidence intervals, stated at the 95 % confidence level,
242 as a measure of precision. The arithmetic mean values for flux and reten-
243 tion measurements were determined based on the taken samples, and the
244 related confidence intervals were calculated. As result there is a 95 % proba-
245 bility that such an estimated interval contains the real value. Furthermore,
246 intervals with a breadth of one (estimated) standard deviation (1σ) are re-
247 ported to relate the obtained data points to the probabilistic distribution of
248 measured values. The smaller the interval, the more narrow is the expected
249 distribution.

250 Obvious single outliers and failed tests had to be identified and removed
251 from the database prior to the statistical evaluation. Failed tests were rec-
252 ognized by an overall visible lower retention or a significantly higher flux
253 value compared to the parallel tested module. They could occur by sealing
254 problems (leak flux) inside the membrane module, membrane defects or con-
255 tamination of the samples before analyzing. These tests were repeated to get

256 a reliable database with minimum 18 raw data points for every single pure
 257 solvent flux and nine raw data points for retention of each molecular weight.
 258 The amount of samples arose from the number of parallel tested membranes
 259 and contributors with the assumption of one failed test. For flux measure-
 260 ments this number were doubled since higher deviations were expected. In
 261 total, this approach generated at least 81 data points for retention curves
 262 measured in ethanol and 90 data points for retention curves measured in
 263 toluene.

264 The calculation of the standard deviation and the confidence intervals
 265 was based on the assumption that the given samples (data points) are un-
 266 biased, independent and statistically normally distributed [35]. Further we
 267 had to notice that the original variance is unknown. Hence, the variance s^2
 268 with the unbiased sample variance arise from:

$$s^2 = \frac{1}{n-1} \sum (x_i - \bar{x})^2 \quad (2)$$

269 n is the number of measurements, x_i , and \bar{x} are the individual measured
 270 values and the related mean value, respectively. The standard deviation σ
 271 is accordingly the square root of the variance s^2 . Due to the limited sample
 272 size, the confidence interval calculation uses the student's t-distribution, con-
 273 sidering the $(1 - \alpha/2)$ quantile of t . The quantile is tabled in the literature
 274 [36]. Thus, the confidence intervals result from:

$$\left[\bar{x} - t_{(1-\alpha/2)} \frac{s}{\sqrt{n}}; \bar{x} + t_{(1-\alpha/2)} \frac{s}{\sqrt{n}} \right] \quad (3)$$

275 With this way of calculation, the range of reliable mean values is de-
 276 termined. Confidence intervals from future experiments can overlap and

277 therefore narrow the range in regard to a real value. However, the primary
278 objective of this study is to define a standard experimental procedure and
279 perform a statistical analysis of the obtained results, allowing for a repre-
280 sentative retrospective on reported data in literature. The effort of the con-
281 tributors to generate comparable results become apparent in the standard
282 deviations of the data points. Assuming an exact normal distribution of the
283 measurement data, reflecting random differences of the membrane material
284 (e.g. thickness of the active layer) it is expected that 95% of all measure-
285 ments will be located in the vicinity of the interval with 2σ range around the
286 real mean. Thus, almost all of the measurements should be located within
287 a range of two (estimated) standard deviation, around a value within the
288 confidence interval of the mean.

289 In addition, tests of normality evidenced the assumption of statistic nor-
290 mally distributed data. The gathered results were tested on normal dis-
291 tribution with the methods of Anderson-Darling (a Goodness-of-Fit-Test)
292 [37, 38] and Shapiro-Wilk (an omnibus test) [39–41]. The Shapiro-Wilk-Test
293 analyzes the variance. Data are normally distributed if the estimated vari-
294 ance is near the hypothetical variance of the normal distribution. With the
295 Anderson-Darling-Test data are sorted and transformed into a uniform dis-
296 tribution. The distance to the hypothetical normal distribution is, in this
297 case, the critical value. Normal distribution was granted if the results passed
298 both sensitive tests.

299 The bilateral cooperative test systems cannot be compared in this way,
300 since only two contributors measured the data. In these cases, minimum
301 four data points are available, which is too few for a reasonable calculation

302 of confidence intervals. The results comply with our claims if the deviation
303 of each data point to the related ones is less or equal than the deviation
304 between the data points in the round robin tests.

305 *4.1. Superstructure optimization*

306 In order to evaluate the effect of the extent of uncertainty related to the
307 experimentally determined performance metrics, different scenarios are eval-
308 uated within a superstructure optimization approach considering a sampling
309 within the ranges of the determined confidence intervals around the estimated
310 mean values. The superstructure represents a so-called state-space approach
311 [42] and builds on a previous implementation for the optimization of reverse
312 osmosis processes for seawater desalination [43]. Similar superstructures have
313 been used for the optimization of gas permeation processes for natural gas
314 upgrading [44] and nitrogen removal from natural gas [45].

315 An illustration of the superstructure, which consists of a generic distri-
316 bution network and three OSN membrane stages is provided in Figure 3. The
317 distribution network allows distribution of the entering streams, which are
318 the overall feed stream and all product streams from the membrane stages, to
319 all outgoing streams that are the feed streams of the OSN stages and the final
320 permeate and retentate product streams. Thereby any kind of combination
321 between the different membrane stages is possible. The performance of each
322 membrane stage is modeled based on the available performance metrics from
323 the experimental data, which are an overall flux as well as solute-specific
324 retention. Furthermore, a concretization of the membrane stage concerning
325 100 finite elements is performed to account for the composition changes along
326 the membrane length.

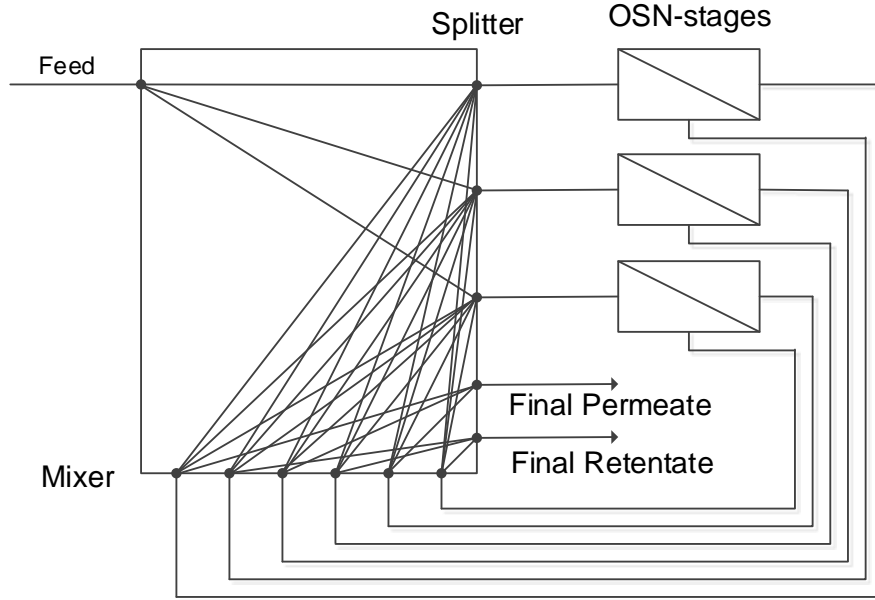


Figure 3: Superstructure for membrane network optimization.

327 However, a constant performance regarding the experimentally deter-
 328 mined values is assumed, and concentration polarization and pressure drop
 329 are neglected since no information on module geometry and hydrodynam-
 330 ics is considered. Operating temperature and pressure are also fixed to the
 331 experimental conditions, such that only the membrane area remains as a de-
 332 gree of freedom for every membrane stage. For the current study a maximum
 333 membrane area of 50 m^2 per stage and a total of three possible stages was
 334 considered. The objective of the optimization is to perform a specific sepa-
 335 ration, concerning purity and recovery constraints, with a minimum number
 336 of membrane stages and membrane area.

337 The superstructure optimization model is implemented in the general
338 modeling framework GAMS as a mixed integer nonlinear programming prob-
339 lem (MINLP). The discrete decisions account for the existence of the dif-
340 ferent membrane stages, for which additional Big-M constraints enforce a
341 minimum feed flowrate for existing membranes, while further constraints
342 introduce additional cuts to eliminate topologically equivalent solutions by
343 enforcing a specific order on the available membrane stages [43]. This is
344 important to avoid multiplicity of equivalent optima in the solution space,
345 which severely complicates global deterministic optimization. The result-
346 ing MINLP is solved using the global deterministic solver ANTIGONE to
347 determine the best possible solution.

348 **5. Results and Discussion**

349 Considering the spent effort devoted to the standardized experimental
350 procedure and the validation of the analytic methods, it can be concluded
351 that the obtained results of the round robin test are a best case representa-
352 tive for the diversity of measurements in diverse laboratories. Differences are
353 quite normal since locations, set-ups, measurement devices, analytic meth-
354 ods, time of measurements and experimenter vary from each other. The
355 contributors endeavored to operate as equal as possible to ensure that the
356 experimental procedure became a standard in functional membrane charac-
357 terization.

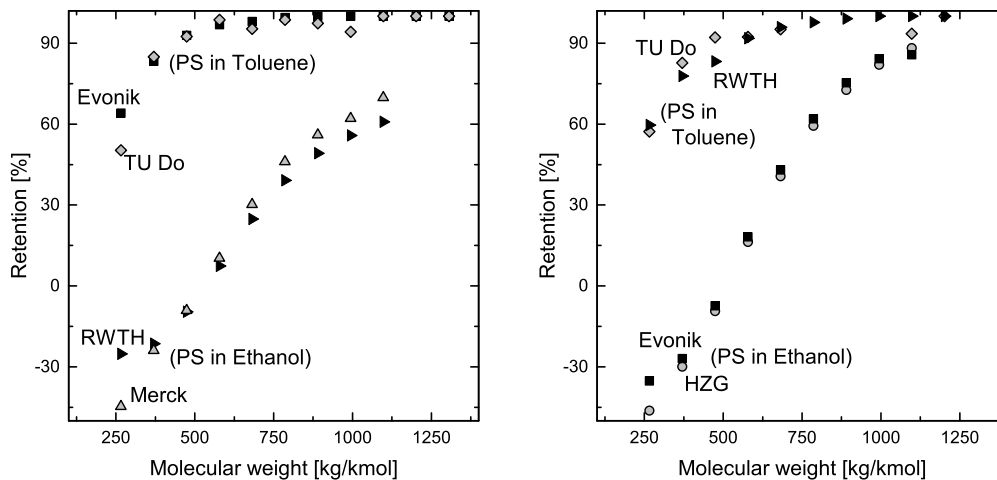
358 *5.1. Comparison of analytic methods*

359 Testing identical samples in different laboratories resulted in a minimal
360 data points variation. Figure 4 shows two diagrams with four exemplary re-

361 retention curves for the comparison of the analytical methods at different lab-
362 oratories. The retention of the different styrene oligomers is plotted versus
363 their molecular weight. Single occasional outliers could be identified by com-
364 paring the curves. The reason for the apparent deviations at 266 kg kmol^{-1}
365 was the more sensitive evaluation of the small peaks obtained by analyzing
366 the retentate and permeate samples. The biggest differences between the
367 measured retention values, excluding outliers are only about 6%, proving
368 the comparability of the analytic methods.

369 5.2. Pure solvent flux

370 Figure 5a shows the results plotted in a box plot (left part for toluene
371 fluxes, right part for ethanol fluxes) for each membrane to display the dis-
372 tribution and differences of the data. Toluene fluxes could be measured only
373 with PuraMem[®] S600 and PDMS membranes. DuraMem[®] series mem-
374 branes showed very low or no permeation with toluene. Ethanol fluxes, how-
375 ever, were measured with all selected membranes. One point worthy of note,
376 is the different scales on the flux axes. Figure 5b illustrates the meaning of
377 the boxplots, in which the dots represent the measured fluxes while the white
378 boxes indicate the standard deviation as 1σ interval of the measured data.
379 The accompanying percentage gives the difference from the arithmetic aver-
380 age to the upper or lower value of the range. Inside the boxes the line and
381 the dot are the median and the arithmetic average of the data respectively.
382 Above and below, the whiskers show the 2σ interval. The grey colored boxes
383 represent the calculated confidence intervals (Eq. 3). The horizontal spread
384 of the data dots is plotted this way to avoid overlap of too many points for
385 the same membrane. It is randomized and has no physical meaning.



(a) Retention measurements with the PDMS membrane.

Evonik ■ and TU Do ◇ used samples with toluene as solvent (sampling at 30 bar).

Merck △ and RWTH ► used samples with ethanol as solvent (sampling at 30 bar).

(b) Retention measurements with the PuraMem® S600.

TU Do ◇ and RWTH ► used samples with toluene as solvent (sampling at 20 bar).

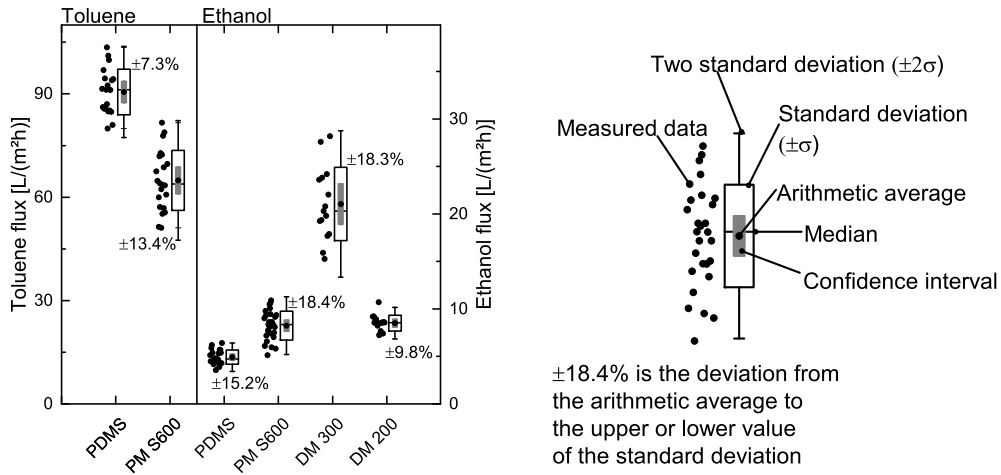
Evonik ■ and HZG ○ used samples with ethanol as solvent (sampling at 40 bar).

Figure 4: Comparison of analytic results from retention measurements with the PDMS membrane and PuraMem® S600

386 The fluxes (Figure 5a) for toluene are much higher than for the polar
 387 solvent ethanol. Highest fluxes with few scattering were measured for the
 388 PDMS membrane. The mean could be found at $90.5 \text{ L m}^{-2} \text{ h}^{-1}$ and the cor-
 389 responding confidence interval is close to this value with $\pm 3.1 \text{ L m}^{-2} \text{ h}^{-1}$. The
 390 standard deviation has limits at $\pm 7.3\%$ of the mean. The results from the
 391 flux measurements with the PuraMem® S600 membrane show wider scatter-
 392 ing with an arithmetic average of $64.9 \text{ L m}^{-2} \text{ h}^{-1}$. However, the breadth of

393 the 1σ interval is $\pm 13.4\%$ of the mean and the measured data shows that
 394 only single higher and lower values lead to the comparative high deviation.
 395 The precision around the estimated mean value amounts to $\pm 3.8 \text{ L m}^{-2} \text{ h}^{-1}$.

396 The toluene fluxes correspond to the expectations of the manufactur-
 397 ers. The higher fluxes through the PDMS membrane compared to those
 398 through the PuraMem[®] S600 membrane can be attributed to the struc-
 399 ture and material of the membranes. The selective layer of the PDMS
 400 membrane consists of radiationally crosslinked PDMS with a thickness of
 401 $2 \mu\text{m}$ [46]. The high toluene fluxes were expected due to the small dis-
 402 tance of the total Hansen Solubility Parameters (HSP) according to [16]
 403 ($|\delta_{\text{Membrane}} - \delta_{\text{Solvent}}| = 2.73 \text{ MPa}^{0.5}$ with $\delta_{\text{Membrane}} = 15.57 \text{ MPa}^{0.5}$ for
 404 PDMS). The coated silicone-based layer of the PuraMem[®] S600 membrane



(a) Box plot and data points of pure solvent fluxes of toluene (left) and ethanol (right) at 30 bar transmembrane pressure and $25 \text{ }^\circ\text{C}$.

(b) Meaning behind the symbols, boxes, whiskers and numbers of the box plots.

Figure 5: Results of pure solvent flux measurements illustrated as box plot.

405 is thin and supported by a polyimide structure. This supporting structure
406 is much more polar than PDMS and seems to have an inhibitory effect on
407 the nonpolar solvent. Accordingly, no flux measurement through the cross-
408 linked polyimide-based membranes DuraMem[®] 300 or DuraMem[®] 200 with
409 toluene was possible.

410 Fluxes of ethanol are mostly around or below $10 \text{ L m}^{-2} \text{ h}^{-1}$. The lowest
411 fluxes were measured with the PDMS membrane and the PuraMem[®] S600
412 membrane with mean values at $4.9 \text{ L m}^{-2} \text{ h}^{-1}$ and $8.2 \text{ L m}^{-2} \text{ h}^{-1}$, respectively.
413 The limits of their 1σ intervals are around $\pm 15.2\%$ and $\pm 18.4\%$. Re-
414 sults from the confidence interval calculation show a difference from the
415 mean value of $\pm 0.3 \text{ L m}^{-2} \text{ h}^{-1}$ for PDMS membrane and $\pm 0.6 \text{ L m}^{-2} \text{ h}^{-1}$ for
416 PuraMem[®] S600 membrane. There is a remarkable deviation in the flux
417 values of the DuraMem[®] 300 membrane. The reason for it is most likely
418 the higher porosity of the membrane and its natural deviation from the pro-
419 duction process. The standard deviation interval is $\pm 18.3\%$ of the mean
420 which is $21.1 \text{ L m}^{-2} \text{ h}^{-1}$. For this case, the confidence interval was deter-
421 mined at $\pm 2.1 \text{ L m}^{-2} \text{ h}^{-1}$. The measurements with the DuraMem[®] 200 mem-
422 brane resulted in a mean value of $8.5 \text{ L m}^{-2} \text{ h}^{-1}$ and a confidence interval of
423 $\pm 0.4 \text{ L m}^{-2} \text{ h}^{-1}$. The standard deviation has limits at $\pm 9.8\%$ of the mean.
424 For all membranes the median is close to the mean. The highest differences
425 are $-1.1 \text{ L m}^{-2} \text{ h}^{-1}$ for toluene flux through the PuraMem[®] S600 membrane
426 and $-0.7 \text{ L m}^{-2} \text{ h}^{-1}$ for ethanol flux through the DuraMem[®] 300 membrane.

427 Furthermore, Figure 5a shows referring to the measurements in ethanol
428 with the PuraMem[®] S600 membrane more data points than for the other
429 measurements. The reason is testings about a reasonable size of the database.

430 For the membrane were additional measurements conducted, so the number
431 of data points rises from 19 to 28. The arithmetic mean value changed slightly
432 (from $8.3 \text{ L m}^{-2} \text{ h}^{-1}$ to $8.2 \text{ L m}^{-2} \text{ h}^{-1}$). The initial 1σ interval decreased as
433 expected from ca. $\pm 18.6\%$ to $\pm 15.2\%$. The additional measurements show
434 the dependency of the data gathered on the number of samples. It is evident
435 that the chosen number of samples is sufficient. On the one hand it is high
436 enough to calculate reasonable standard deviations and confidence intervals.
437 On the other hand it is small enough to avoid inefficiency and insignificant
438 interval ranges.

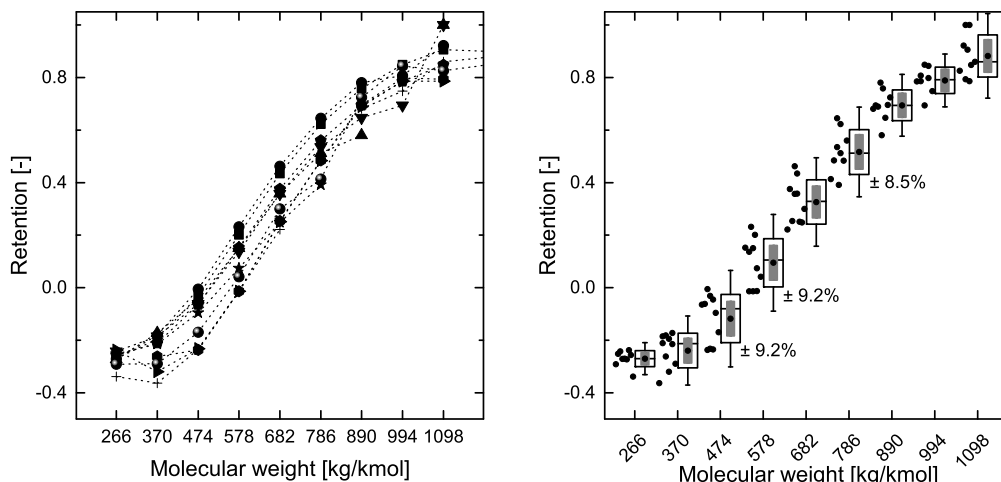
439 The fluxes of ethanol through the membranes match the expectations
440 of the manufacturers. The fluxes are significantly lower, depending on the
441 material of the active membrane layer. As a second factor, the degree of
442 cross-linking and thus the tightness of the membrane is essential. It is chal-
443 lenging for polar substances, such as ethanol, to permeate through the two
444 nonpolar silicone-based membranes. This low permeation results in the low-
445 est fluxes for the PDMS membrane and only slightly higher values for the
446 coated PuraMem[®] S600 membrane. In contrast to the flux measurements
447 with toluene, the polyimide substructure of the PuraMem[®] S600 membrane
448 allows a higher liquid flux for ethanol.

449 Besides, it is interesting to note that the flux through the PuraMem[®] S600
450 membrane corresponds approximately to that through the DuraMem[®] 200
451 membrane. According to the manufacturer, the DuraMem[®] 200 membrane
452 has a lower MWCO than the PuraMem[®] S600. It is evident that the silicone-
453 based coating (active membrane layer) appropriately hinders the permeation
454 of the polar solvent, since the supporting structure of the PuraMem[®] S600

455 membrane (produced of the same material as the DuraMem[®] 200) is less
456 cross-linked and, therefore, consists of a more open structure.

457 The observed standard deviations of the measured flux values show that
458 distinct differences can occur in the measurements, despite the standard-
459 ized procedure. These differences can be observed especially for pure solvent
460 fluxes. However, the differences also confirm the experience of the mem-
461 brane manufacturers. As already mentioned for the DuraMem[®] 300, one
462 possible origin of the deviations are the production tolerances that occur
463 within a batch. It should also be remembered that the membranes in labo-
464 ratory plants have a much smaller surface area. The membrane sample can
465 only show an average value corresponding to the large production batches
466 or modules if they either represent precisely the average of the batch or are
467 measured in sufficient numbers. The low confidence intervals in combina-
468 tion with the close range of median and arithmetic mean demonstrate that
469 the results provide highly precise information on flux averages. This study
470 is unique in that the measurements were carried out at different times in
471 different institutions. The comparison between measurements of laboratory
472 size membranes and industrial membrane modules is an interesting topic for
473 future work.

474 The summary is based on 136 measurement data points, whereby 12 out-
475 liers were excluded. The breadths of all 1σ intervals are lower than $\pm 20\%$.
476 Also, the mean values were estimated with a high precision. The results ver-
477 ify the reliability of the proposed standard experimental procedure for flux
478 measurements.



(a) Array of all measured retention curves from the round robin test with polystyrene oligomers in ethanol with the PDMS membrane. A different symbol is used for each measurement series. Obvious outliers are removed.

(b) Box plot and measured data points from the round robin test with polystyrene oligomers in ethanol with the PDMS membrane.

Figure 6: Results from the round robin test with the PDMS membrane and polystyrene in ethanol at 30 bar transmembrane pressure and 25 °C.

479 5.3. Retention measurement

480 To visualize the retention measurements, we depict the results of the
 481 round robin tests in two ways (Figure 6). Figure 6a shows the array of reten-
 482 tion curves for this test system, whereby the outliers are already excluded.
 483 The outliers were identified only with the help of the regular retention curves
 484 (the points were laying clearly outside of the curve). These outliers could
 485 also have an analytical background as previously shown in Figure 4. Only six
 486 outliers out of 90 data points were identified for the system PDMS membrane-
 487 ethanol-polystyrene. The results can therefore be seen as representative. The

488 curves are forming a belt, starting with a negative retention for the smaller
489 molecules and ending with a retention of above 90 % for the bigger styrene
490 oligomers, as expected. The experimental data points for the retention of
491 each styrene (different molecular weight) adhere to a normal distribution,
492 with the exception of the high retention values of large oligomers ($R > 97\%$),
493 due to the upper limit of 100 % retention. Consequently, outliers for such
494 molecular weights are irrelevant for the results evaluation too.

495 The second depiction (Figure 6b) displays the relevant retention of the
496 different oligomers (different molecular weight) in box plots similar to Fig-
497 ure 5b. In such diagrams, it is easier to visualize the distribution of the
498 results. Figure 6b shows exemplary the box plots for the PDMS-membrane
499 in ethanol, Figure 7 shows the plots for the DuraMem[®] 300 membrane also
500 in ethanol and Figure 8 shows the plots for the PuraMem[®] S600 membrane
501 in toluene.

502 The values on the horizontal axis are the molecular weights from the sin-
503 gle styrene oligomers. They could be identified analytically with 266 kg kmol^{-1}
504 $+ n \cdot 104 \text{ kg kmol}^{-1}$. The boxes positions are following the retention curves.
505 While the boxes from the system PDMS membrane-ethanol-polystyrene show
506 the described increase of retention with increasing molecular weight of the
507 oligomers, the boxes of the system DuraMem[®] 300 membrane-ethanol-polystyrene
508 form a horizontal line above 90 % retention (Figure 7). Fewer oligomers
509 could be considered in this system because of the proximity to the retention
510 limit and the smaller MWCO in this solvent-solute combination. The sys-
511 tem PuraMem[®] S600 membrane-ethanol-polystyrene (not depicted) behaved
512 similarly as the system PDMS membrane-ethanol-polystyrene. The results

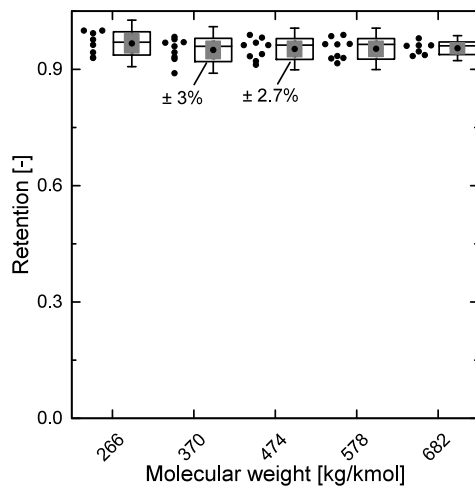


Figure 7: Box plot and data points of retention values from the round robin test with the DuraMem[®] 300 and polystyrene in ethanol at 30 bar transmembrane pressure and 25 °C.

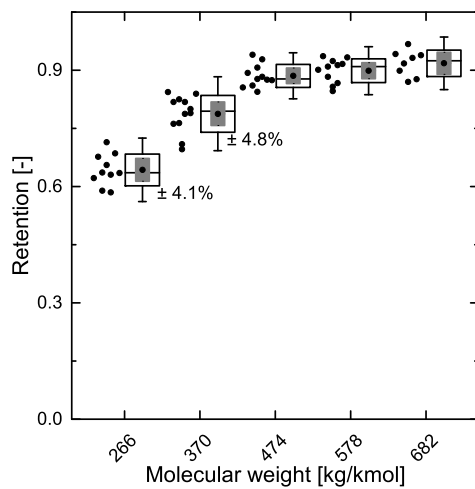


Figure 8: Box plot and data points of retention values from the round robin test with the PuraMem[®] S600 and polystyrene in toluene at 30 bar transmembrane pressure and 25 °C.

513 from the PuraMem[®] S600 membrane-toluene-polystyrene experiments (Fig-
514 ure 8) shows boxes positions from characteristic retention curves as well.
515 The increase of the retention values for the different styrene oligomers is
516 more gradual as 60 % retention was already achieved for the smallest styrene
517 oligomer. In this case, the system PDMS membrane-toluene-polystyrene (not
518 depicted) behaved similarly. The retention values in all these systems were
519 affected by the different pressure level only slightly. Changes primary oc-
520 curred for the lower retention values. Positive retention values increased by
521 increasing pressure while negative retention values decreased by increasing
522 pressure. Regarding the scattering of the data points, no tendency could be
523 mentioned. At first glance, the measurements seem to be comparable.

524 The results prove the good applicability of the developed standard testing
525 procedure. All 1σ intervals have a low absolute range. The highest breadth
526 is $\pm 9.2\%$ of the mean value at the test system PDMS membrane-ethanol.
527 Even with Figure 9 it becomes apparent that all measured curves are within
528 or close to the calculated confidence intervals. The intervals are drawn as
529 retention curves and superimposed on the array of measured data. Thus, it
530 shows in another way the precision of the results and the quality of a stan-
531 dardized experimental procedure.

532 The measured retentions are in line with the expectations of the mem-
533 brane manufacturers. The results show that the gradient of the retention
534 curves is dependent on the membrane for low molecular weight solutes.
535 Oligomers with a higher molecular weight can only permeate to a small ex-
536 tent because of their high diffusion coefficients. The gradient at low molecular
537 weights is highest in both toluene and ethanol for the PDMS membrane and

538 lowest for DuraMem[®] 300 membrane in ethanol. Here the interactions be-
539 tween membrane, solute and solvent are the major factors.

540 The nonpolar polystyrenes dissolve and permeate preferably through non-
541 polar membranes. However, increasing numbers of polar groups in a mem-
542 brane, such as the DuraMem[®] 300 membrane, lead to a stronger permeation
543 barrier. Concurrently, the nonpolar solutes can interact less with the polar
544 ethanol than with the nonpolar toluene. These effects result in very high re-
545 tentions even for low molecular weight oligomers using the DuraMem[®] 300
546 membrane. The high retentions are also supported by the dense membrane
547 structure indicated in the manufacturers' MWCO specification.

548 The PDMS membrane, on the other hand, impedes permeation of the
549 solvent ethanol rather than of the polystyrene. This preferential permeation
550 leads to negative retentions for the low molecular weights. With increasing
551 molecular weight, the steric effect of the molecules increases and leads to
552 an increase in retention. Since a gradual increase can also be observed in
553 toluene, it can be assumed that the steric factors of the molecules are dom-
554 inant. This conclusion also corresponds to the statement from Thiermeyer
555 et al. [46].

556 The polystyrenes have a high affinity to the PuraMem[®] S600 mem-
557 brane due to the nonpolar coating. However, the affinity is weakened by
558 the supporting structure. The same applies for the solvent toluene as de-
559 scribed for the pure solvent fluxes. Therefore, toluene also provides higher
560 retention for polystyrene oligomers with a lower molecular weight using the
561 PuraMem[®] S600 membrane compared to the PDMS membrane. Similar
562 to this membrane, the importance of steric effects increases with increasing

563 molecule size. In ethanol, it is contrary for the solvent, and the nonpolar
564 silicone-based layer hinders the flux through the membrane. These measure-
565 ments showed negative retentions which were also observed for the PDMS
566 membrane.

567 From the statistical evaluation, it can be seen that the results show less
568 deviations compared to the pure solvent fluxes. The standard deviation is
569 low and the distance between median and arithmetic mean is small. The
570 low confidence intervals demonstrate that the standardized procedure pro-
571 duces precise estimates of the mean value. Accordingly, it can be assumed
572 that similar results will be achieved with retention measurements using the
573 standardized procedure. Meaning that a few measurements per solute are
574 sufficient for the characterization of a new membrane.

575 The retention results from the bilateral cooperative tests (performed par-
576 allel by two contributors) were compared directly for each molecular weight.
577 Since there were only four data points for the retention of each solute, con-
578 fidence intervals were not considered and no standard deviations were calcu-
579 lated. Figure 10 shows the retention of alkanes and SOA as well as PMMA
580 in different solvents.

581 The depicted retention curves of alkanes and SOA were results from mea-
582 surements with the PDMS membrane. In isopropyl alcohol (IPA) and ethyl
583 acetate (ESTP) negative retention occur. With increasing molecular weight,
584 the retention values decrease in the polar solvent IPA, whereas increase in
585 the moderate polar solvent ESTP. As mentioned above, such negative reten-
586 tions were also observed in some measurements with styrene oligomers. In
587 the nonpolar solvent n-heptane, the measurements with alkanes resulted in

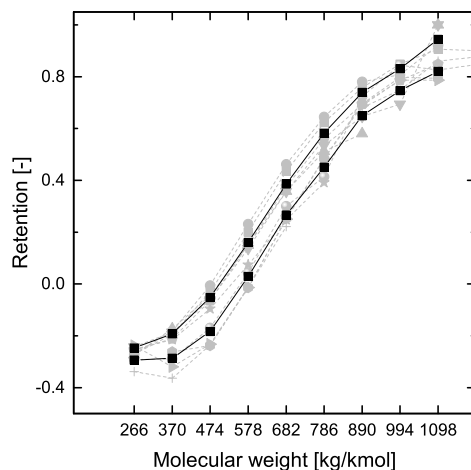
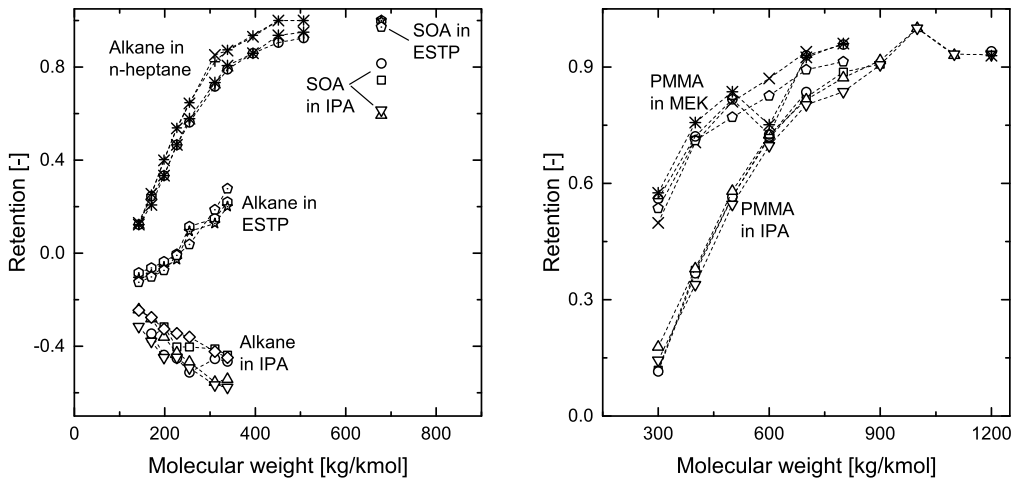


Figure 9: Calculated confidence intervals (■) drawn as retention curves. They are superimposed on the array of measured retention curves from the round robin test with the PDMS membrane and polystyrene in ethanol at 30 bar transmembrane pressure and 25 °C. A different symbol is used for each measurement series.

588 only positive values as common retention curves. Affinity effects established
 589 with solubility parameter could give an explanation about this behaviour.
 590 Similar measurements and results were presented in Postel et al. [16]. SOA
 591 is a more complex branched molecule with a higher molecular weight than
 592 the alkanes. Consequently, it can be argued that the diffusion coefficient is
 593 high compared to that of the alkanes. Furthermore, SOA is a moderately
 594 polar solute with a high acceptance for hydrogen bonds due to its excellent
 595 water solubility and the bounded oxygen. This polarity leads to the assump-
 596 tion of a high Hansen Solubility Parameter. For that reason a low affinity
 597 to the nonpolar PDMS membrane is expected. In this combination, similar
 598 to the polyethylene glycol retention in Postel et al. [16], the size exclusion is
 599 dominant for retention in IPA and ESTP (SOA is not soluble in n-heptane).

600 The retention measurements of PMMA oligomers with PuraMem[®] S600
 601 membranes (Figure 10b) results in common retention curves. The mea-
 602 surements with the combination butanone (MEK) and PMMA results in
 603 higher retention values than the measurements with the combination IPA
 604 and PMMA. Such lower retention values in IPA could also lead back to affin-
 605 ity effects, since the active layer of the PuraMem[®] S600 membrane is silicon
 606 based as the PDMS membrane.

607 The curves in both diagrams are not corrected and the plausible outliers
 608 are easily recognizable (retention curves of PMMA in butanone (MEK) or
 609 SOA in IPA). The total deviation in retention for each solute is, however, as



(a) Retention curves of alkane and SOA in various solvents at 30 bar transmembrane pressure and 25 °C for the PDMS membrane.

(b) Retention curves of PMMA in IPA and MEK at 30 bar transmembrane pressure and 25 °C for the PuraMem[®] S600 membrane.

Figure 10: Results from additional tests distributed to two contributors each. A different symbol is used for each measurement series.

610 low as the one in the round robin test. Most of the data points deviate by
611 less than 10% in total, and every deviation is in total less than $\pm 15\%$ of the
612 arithmetic average.

613 5.4. Case studies

614 Two different case studies were investigated using the superstructure opti-
615 mization approach to elucidate the effect of uncertainties of flux and retention
616 measurement on subsequent process design. In Case Study 1 a concentra-
617 tion of one component with a molecular weight of 474 kg kmol^{-1} solved in
618 ethanol is assessed, considering the experimentally determined performance
619 metrics of the DuraMem[®] 300 membrane and the mixture of ethanol with
620 styrene oligomers. The flux across the membrane at 30 bar was determined
621 to $21.052 \text{ L m}^{-2} \text{ h}^{-1}$ while the confidence interval was $\pm 2.136 \text{ L m}^{-2} \text{ h}^{-1}$. The
622 retention for the styrene oligomer with a molecular weight of 474 kg kmol^{-1}
623 was determined to $95.2\% \pm 2.1\%$.

624 For the optimization a feed flowrate of 100 kg h^{-1} , a concentration from
625 0.05 g g^{-1} in the feed to 0.1 g g^{-1} in the final retentate and a solute recovery
626 of at least 98% was assumed.

627 Figure 11 shows three of the resulting optimal process structures, for
628 exemplary samples within the experimentally determined confidence inter-
629 vals. Depending on the selected case, significant differences in the necessary
630 membrane area and the complexity of the process arise. While the high flux
631 and retention values lead to a simple process in a single step, the process with
632 the low values is much more complicated and not intuitive. The total feed is
633 divided between a parallel module and a two-stage cascade. The permeate
634 flow of the first stage is only partially used for the second cascade stage.

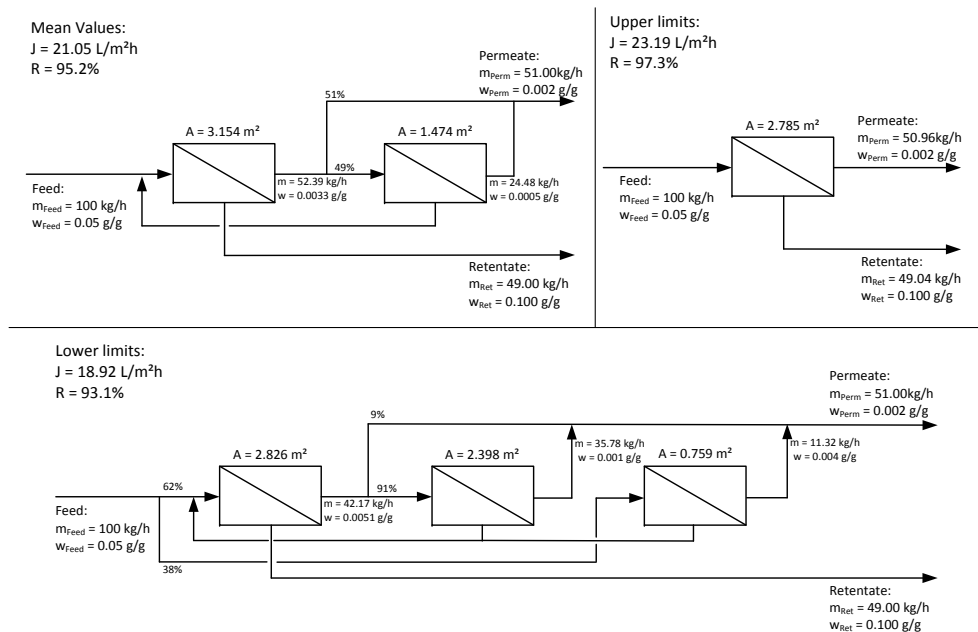


Figure 11: Case study 1: Three optimized process structures for different flux and retention combinations from the test system DuraMem[®] 300-ethanol-polystyrene ($M_w = 474 \text{ kg kmol}^{-1}$) at 30 bar and 25 °C.

635 The retentate streams from the module operated in parallel and the second
 636 cascade stage are fed back to the feed of the cascade, before the first stage.
 637 Output streams from the process are the retentate stream from the first cas-
 638 cascade stage and the combined permeate streams from all membrane modules.
 639 Overall nine different scenarios were evaluated, for which the supplemental
 640 file provides the performance metrics and the key structural results, regard-
 641 ing the number of required stages and overall membrane area.

642 As a second case study, a separation step of two solutes solved in ethanol
 643 was chosen. The solute size equals 474 kg kmol^{-1} and $1098 \text{ kg kmol}^{-1}$. The

644 smaller solute is assumed to be the product while the bigger solute represents
645 an impurity. The feed contains 0.05 g g^{-1} of the product and 0.003 g g^{-1} of
646 the impurity while the flow rate is set to 100 kg h^{-1} . The final permeate needs
647 to contain at least 98 % of the product, and the concentration of the impurity
648 in the permeate needs to be lower than 0.001 g g^{-1} . For this case study, the
649 experimental values determined with the PDMS membrane and the mixture
650 of ethanol with styrene oligomers are used. The flux was experimentally de-
651 termined to be $4.925 \text{ L m}^{-2} \text{ h}^{-1} \pm 0.331 \text{ L m}^{-2} \text{ h}^{-1}$ at 30 bar. The retention of
652 the styrene oligomer with a molecular weight of 474 kg kmol^{-1} equals -11.8%
653 $\pm 6.6 \%$ and the retention of the styrene oligomer with a molecular weight of
654 $1098 \text{ kg kmol}^{-1}$ equals 88.2% $\pm 6.2 \%$.

655 Compared to the first case study the flux is much smaller, and addition-
656 ally, the experimentally determined confidence intervals are broader. Overall
657 27 different combinations of flux and retentions were evaluated, all of which
658 represent samples within the ranges of the experimentally determined confi-
659 dence intervals. Three of the determined optimal process structures for the
660 second case study are depict in Figure 12. This case study also shows clear
661 differences in the necessary membrane area and the interconnection concepts.
662 The value combination of high flux and retentions far from each other lead
663 to a simple single-stage membrane process with a small membrane area. On
664 the other hand, lower flux values and a narrower retention range between the
665 individual solutes result in a substantially more complex two-stage process.
666 In this process, the main feed is divided between the two stages, with part of
667 the permeate from the first stage supplementing the feed of the second stage.
668 The feed of the first stage is also fed with the retentate of the second stage.

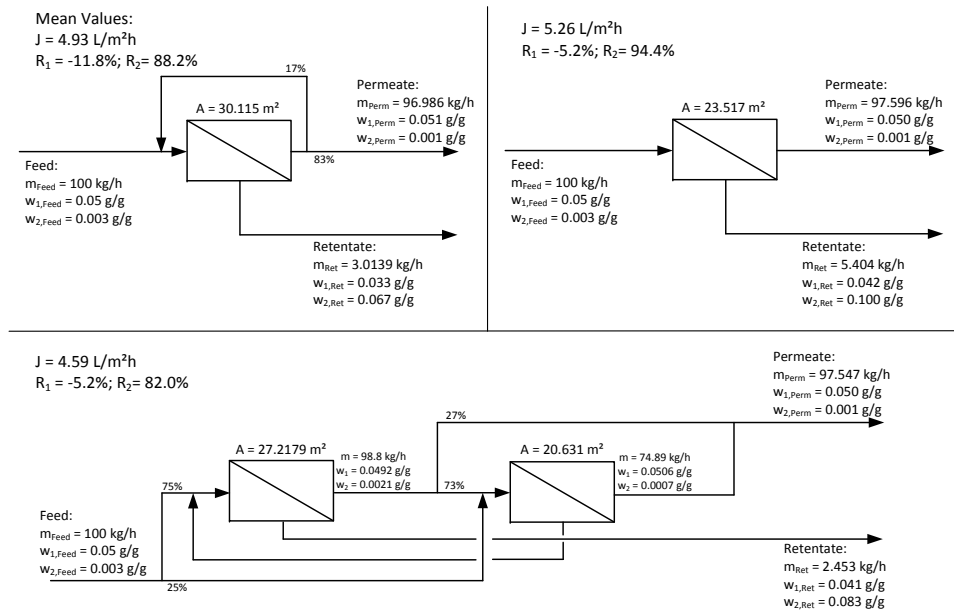


Figure 12: Case study 2: Three optimized process structures for different flux and retention combinations from the test system PDMS membrane-ethanol-polystyrene ($M_w = 474 \text{ kg kmol}^{-1}$ as product and $1098 \text{ kg kmol}^{-1}$ as impurity) at 30 bar and 25°C .

669 The output streams are the retentate of the first stage and a mixture of the
 670 permeates of the two stages. A summary of the results for the second case
 671 study is listed in the supplemental data.

672 Both case studies demonstrate the dependency of a subsequent process
 673 design on accurate information of the membrane performance. A consistent
 674 determination and reporting of the data quality, as indicated in the current
 675 study, is, therefore, an essential component for the further development and
 676 dissemination of OSN processes.

677 **6. Conclusion**

678 The data quality of results from membrane characterizations has never
679 been stated as a basis for the OSN users. This uncertainty hinders the
680 progress in finding one or more reasonable standard systems for OSN mem-
681 brane characterization. Such standardized procedure can simplify the as-
682 sessment of membrane performance and their applicability in real separation
683 processes. As a result, the process design of a OSN plant in industrial scale
684 would be less difficult and troublesome.

685 In this study, we demonstrate the reliability and reproducibility of a stan-
686 dardized experimental procedure to improve and accelerate process design for
687 OSN applications. The procedure was applied with different test and ana-
688 lytical equipment, for several solvents, membranes, and solutes.

689 The results from the round robin test were statistically evaluated. The
690 calculations for pure solvent flux and retention measurements demonstrate
691 that the precision of the determined mean values from the experiments are
692 high and the standard deviations reasonable. Therefore, the deviation of the
693 data is low enough to permit the assumption of comparable results in future
694 tests by using the standardized experimental procedure.

695 Using the statistically quantified information on the accuracy of the de-
696 termined experimental flux and retention values, we further demonstrated
697 the effect of these uncertainties on subsequent process design. The two in-
698 vestigated case studies confirmed the importance of an accurate assessment
699 of data quality and accuracy. The standardized procedure for membrane
700 characterization experiments should help to assess future results better and
701 apply statistical methods. Then data from different sources and their relia-

702 bility can be used in optimal process design.

703 Further results with other test systems confirm the reliability of the
704 method and emphasize the comparability of the obtained results.

705 Considering all results, we showed that the proposed standard experimen-
706 tal procedure, used in a conjunction with the categorized test systems, enable
707 generating comparable and reliable membrane performance data. Prospec-
708 tively, this procedure can become a standard to characterize OSN membranes
709 and give credible performance information. Nevertheless, further investiga-
710 tion on this field is desirable. A development of heuristic method for mem-
711 brane selection could promote and strengthen the method. Furthermore, it
712 can help with its reliable results to reveal correlations in the complex solvent-
713 solute-membrane system in future work.

714 **Acknowledgment**

715 The authors wish to acknowledge the German Federal Ministry for Eco-
716 nomic Affairs and Energy (BMWi) for financial support via the project "En-
717 ergieeffiziente Stofftrennung in der chemischen und pharmazeutischen Indus-
718 trie durch Membranverfahren - ESIMEM" (03ET1279E).

719 **References**

- 720 [1] A. Linden, J. Fenn, Understanding gartners hype cycles, Strategic
721 Analysis Report N° R-20-1971. Gartner, Inc (2003).
- 722 [2] L. Liu, W. Chen, Y. Li, An overview of the proton conductivity of nafion
723 membranes through a statistical analysis, Journal of Membrane Science
724 (2016).

- 725 [3] P. Marchetti, M. F. J. Solomon, G. Szekely, A. G. Livingston, Molecular
726 Separation with Organic Solvent Nanofiltration : A Critical Review,
727 Chem. Rev. 114 (2014) 10735–10806.
- 728 [4] L. Peeva, M. Sairam, A. Livingston, 2.05 - nanofiltration operations in
729 nonaqueous systems, in: E. Drioli, , L. Giorno (Eds.), Comprehensive
730 Membrane Science and Engineering, Elsevier, Oxford, 2010, pp. 91 –
731 113.
- 732 [5] F. P. Cuperus, Organic solvent nanofiltration applications: from lead
733 to implementation, in: Proceedings of the 5th International Conference
734 on Organic Solvent Nanofiltration, Antwerp, Belgium, 2015, p. 37.
- 735 [6] S. Blumenschein, S. Druwe, U. Kätzel, The first of its kind OSN plant in
736 a specialty chemicals company: a long and rocky journey, in: Proceed-
737 ings of the 5th International Conference on Organic Solvent Nanofiltration,
738 Antwerp, Belgium, 2015, p. 38.
- 739 [7] M. Haverkamp, M. Herbst, J. Stegger, Recent industrial OSN units:
740 From process idea to industrial implementation, in: Proceedings of the
741 6th International Conference on Organic Solvent Nanofiltration, Saint-
742 Petersburg, Russia, 2017, p. 40.
- 743 [8] X. Yang, A. Livingston, L. F. dos Santos, Experimental observations of
744 nanofiltration with organic solvents, Journal of Membrane Science 190
745 (2001) 45 – 55.
- 746 [9] J. Geens, A. Hillen, B. Bettens, B. Van der Bruggen, C. Vandecasteele,
747 Solute transport in non-aqueous nanofiltration: effect of membrane ma-

- 748 terial, *Journal of Chemical Technology & Biotechnology* 80 (2005) 1371–
749 1377.
- 750 [10] H. J. Zwijnenberg, S. M. Dutczak, M. E. Boerrigter, M. A. Hempenius,
751 M. W. J. Luiten-Olieman, N. E. Benes, M. Wessling, D. Stamatialis,
752 Important factors influencing molecular weight cut-off determination of
753 membranes in organic solvents, *Journal of Membrane Science* 390-391
754 (2012) 211–217.
- 755 [11] S. Postel, C. Schneider, M. Wessling, Solvent dependent solute solu-
756 bility governs retention in silicone based organic solvent nanofiltration,
757 *Journal of Membrane Science* 497 (2016) 47–54.
- 758 [12] H. B. Soltane, D. Roizard, E. Favre, Study of the rejection of various so-
759 lutes in osn by a composite polydimethylsiloxane membrane: Investiga-
760 tion of the role of solute affinity, *Separation and Purification Technology*
761 161 (2016) 193 – 201.
- 762 [13] P. Schmidt, T. Köse, P. Lutze, Characterisation of organic solvent
763 nanofiltration membranes in multi-component mixtures: Membrane re-
764 jection maps and membrane selectivity maps for conceptual process de-
765 sign, *Journal of Membrane Science* 429 (2013) 103–120.
- 766 [14] S. R. Hosseinabadi, K. Wyns, V. Meynen, A. Buekenhoudt, B. V.
767 der Bruggen, Solvent-membrane-solute interactions in organic solvent
768 nanofiltration (osn) for grignard functionalised ceramic membranes: Ex-
769 planation via spiegler-kedem theory, *Journal of Membrane Science* 513
770 (2016) 177 – 185.

- 771 [15] D. Stamatialis, N. Stafie, K. Buadu, M. Hempenius, M. Wessling, Obser-
772 vations on the permeation performance of solvent resistant nanofiltration
773 membranes, *Journal of Membrane Science* 279 (2006) 424 – 433.
- 774 [16] S. Postel, G. Spalding, M. Chirnside, M. Wessling, On negative reten-
775 tions in organic solvent nanofiltration, *Journal of Membrane Science*
776 447 (2013) 57–65.
- 777 [17] C. J. Davey, Z.-X. Low, R. H. Wirawan, D. A. Patterson, Molecu-
778 lar weight cut-off determination of organic solvent nanofiltration mem-
779 branes using poly(propylene glycol), *Journal of Membrane Science* 526
780 (2017) 221 – 228.
- 781 [18] X. Li, F. Monsuur, B. Denoulet, A. Dobrak, P. Vandezande, I. F. J.
782 Vankelecom, Evaporative light scattering detector: Toward a general
783 molecular weight cutoff characterization of nanofiltration membranes,
784 *Analytical Chemistry* 81 (2009) 1801–1809.
- 785 [19] J. da Silva Burgal, L. G. Peeva, S. Kumbharkar, A. Livingston, Or-
786 ganic solvent resistant poly(ether-ether-ketone) nanofiltration mem-
787 branes, *Journal of Membrane Science* 479 (2015) 105 – 116.
- 788 [20] Y. H. See Toh, X. X. Loh, K. Li, A. Bismarck, A. G. Livingston, In
789 search of a standard method for the characterisation of organic solvent
790 nanofiltration membranes, *Journal of Membrane Science* 291 (2007)
791 120–125.
- 792 [21] M. Bastin, K. Hendrix, I. Vankelecom, Solvent resistant nanofiltration

- 793 for acetonitrile based feeds: A membrane screening, *Journal of Mem-*
794 *brane Science* 536 (2017) 176 – 185.
- 795 [22] P. Schmidt, E. L. Bednarz, P. Lutze, A. Górak, Characterisation of
796 Organic Solvent Nanofiltration membranes in multi-component mix-
797 tures: Process design workflow for utilising targeted solvent modifica-
798 tions, *Chemical Engineering Science* 115 (2014) 115–126.
- 799 [23] F. P. Cuperus, How to run membrane experiments
800 successfully, Online brochure, 2012. Retrieved from
801 <http://www.solsep.com/Brochures/Pilotplantv21.pdf>.
- 802 [24] B. Shi, P. Marchetti, D. Peshev, S. Zhang, A. G. Livingston, Will ultra-
803 high permeance membranes lead to ultra-efficient processes? challenges
804 for molecular separations in liquid systems, *Journal of Membrane Sci-*
805 *ence* 525 (2017) 35–47.
- 806 [25] P. Marchetti, L. Peeva, A. Livingston, The selectivity challenge in or-
807 ganic solvent nanofiltration: membrane and process solutions, *Annual*
808 *review of chemical and biomolecular engineering* 8 (2017) 473–497.
- 809 [26] S. Keller, G. Korkmaz, M. Orr, A. Schroeder, S. Shipp, The evolu-
810 tion of data quality: Understanding the transdisciplinary origins of data
811 quality concepts and approaches, *Annual Review of Statistics and Its*
812 *Application* 4 (2017) 85–108.
- 813 [27] I. Smallwood, *Handbook of organic solvent properties*, Butterworth-
814 *Heinemann*, 2012.

- 815 [28] C. M. Hansen, Hansen solubility parameters: a user's handbook, CRC
816 press, 2007.
- 817 [29] B. Shi, P. Marchetti, D. Peshev, S. Zhang, A. G. Livingston, Perfor-
818 mance of spiral-wound membrane modules in organic solvent nanofil-
819 tration fluid dynamics and mass transfer characteristics, *Journal of*
820 *Membrane Science* 494 (2015) 8 – 24.
- 821 [30] G. Li, Y. Cai, X. Liao, J. Yin, Enzymatic synthesis of sucrose octaac-
822 etate using a novel alkaline protease, *Biotechnology Letters* 33 (2011)
823 607–610.
- 824 [31] G. Wypych, {PMMA} polymethylmethacrylate, in: G. Wypych (Ed.),
825 *Handbook of Polymers*, ChemTec Publishing, second edition, 2016, pp.
826 467 – 471.
- 827 [32] C. Reichardt, Solvatochromic dyes as solvent polarity indicators, *Chem-*
828 *ical Reviews* 94 (1994) 2319–2358.
- 829 [33] S. Hoffmann, A systematic investigation of transport phenomena in or-
830 ganic solvent nanofiltration, Dissertation, RWTH Aachen, Aachen, 2015.
- 831 [34] M. Razali, C. Didaskalou, J. F. Kim, M. Babaei, E. Drioli, Y. M. Lee,
832 G. Szekely, Exploring and exploiting the effect of solvent treatment in
833 membrane separations, *ACS applied materials & interfaces* 9 (2017)
834 11279–11289.
- 835 [35] E. Walter, L. Pronzato, Identification of parametric models from exper-
836 imental data, Springer Verlag, 1997.

- 837 [36] D. Meintrup, S. Schäffler, Stochastik: Theorie und Anwendungen,
838 Springer-Verlag, 2006.
- 839 [37] T. W. Anderson, D. A. Darling, Asymptotic theory of certain “goodness
840 of fit” criteria based on stochastic processes, Ann. Math. Statist. 23
841 (1952) 193–212.
- 842 [38] M. A. Stephens, Goodness of Fit, AndersonDarling Test of, John Wiley
843 & Sons, Inc., pp. 1–4.
- 844 [39] S. S. Shapiro, M. B. Wilk, An analysis of variance test for normality
845 (complete samples), Biometrika 52 (1965) 591–611.
- 846 [40] P. Royston, Statistical algorithms: Remark AS R94: A remark on
847 Algorithm AS 181: The W -test for normality, j-APPL-STAT 44 (1995)
848 547–551.
- 849 [41] M. M. Rahman, Z. Govindarajulu, A modification of the test of shapiro
850 and wilk for normality, Journal of Applied Statistics 24 (1997) 219–236.
- 851 [42] M. J. Bagajewicz, V. Manousiouthakis, Mass/heat-exchange network
852 representation of distillation networks, AIChE Journal 38 (1992) 1769–
853 1800.
- 854 [43] M. Skiborowski, A. Mhamdi, K. Kraemer, W. Marquardt, Model-based
855 structural optimization of seawater desalination plants, Desalination
856 292 (2012) 30–44.
- 857 [44] M. Scholz, M. Alders, T. Lohaus, M. Wessling, Structural optimization

- 858 of membrane-based biogas upgrading processes, *Journal of Membrane*
859 *Science* 474 (2015) 1–10.
- 860 [45] B. Ohs, J. Lohaus, M. Wessling, Optimization of membrane based nitro-
861 gen removal from natural gas, *Journal of Membrane Science* 498 (2016)
862 291–301.
- 863 [46] Y. Thiermeyer, S. Blumenschein, M. Skiborowski, Solvent dependent
864 membrane-solute sensitivity of osn membranes, *Journal of Membrane*
865 *Science* 567 (2018) 7–17.